

Abstract

Preclinical and clinical studies have demonstrated that plasmid IL-12 (tavokingene telseplasmid) delivered intratumorally via electroporation (TAVO) induces local expression of IL-12p70, converting immunologically excluded tumors into inflamed immunogenic lesions, which is fundamental to generating objective responses in both treated and untreated distant tumors. Recent optimization of electroporation parameters and plasmid design has yielded a significant increase in intratumoral expression and anti-tumor efficacy in preclinical models. To further develop this platform, longitudinal biomarker data from TAVO clinical trials was interrogated to identify key immunological components associated with an effective therapy. This analysis revealed that the composition of TAVO-inflamed lesions, specifically the frequency of CD8+ TIL and the chemokines necessary for their maintenance relative to suppressive intratumoral immune subsets, coincided with clinical responses. We therefore developed a plasmid that encodes both IL-12 and the effector T cell chemokine, CXCL9, which, when transfected into a tumor, are functionally active both *in vitro* as well as *in vivo*, yielding abscopal responses and increased survival.

To further amplify this technology, a strategy was developed to engage the highly relevant and recently described bystander non-tumor reactive T cells in the tumor microenvironment (TME). To accomplish this pan-T cell amplification, a separate therapeutic plasmid encoding membrane-bound anti-CD3 scFv (145-2C11) was used to decorate transfected tumors with the potent polyclonal T cell stimulator. Membrane expression of anti-CD3 *in vivo* was confirmed by immunoblot and flow cytometry. Combination of IL-12/CXCL9 with anti-CD3 delivered by electroporation (collectively, "SPARK") increased both antigen-specific and polyclonal T cells responses, demonstrated by *in vivo* CTL and proliferation assays. Finally, SPARK upregulated the transcription of key immunological genes, leading to regression of both treated and untreated tumors, which heightens its ability to reshape the TME and drive systemic anti-tumor immunity. In conclusion, this data supports a model whereby IL-12 in concert with CXCL9 inflames the lesion, leading to a brisk T cell infiltrate, which in sequence with anti-CD3 stimulation, drives a broad yet robust systemic T cell response. SPARK represents a significant advancement in cytokine-based immunotherapy.

P2A-linked bicistronic IL-12 plasmid (TAVO[®]) delivered via low voltage electroporator (APOLLO) improves therapeutic response in a contralateral B16.F10 tumor model

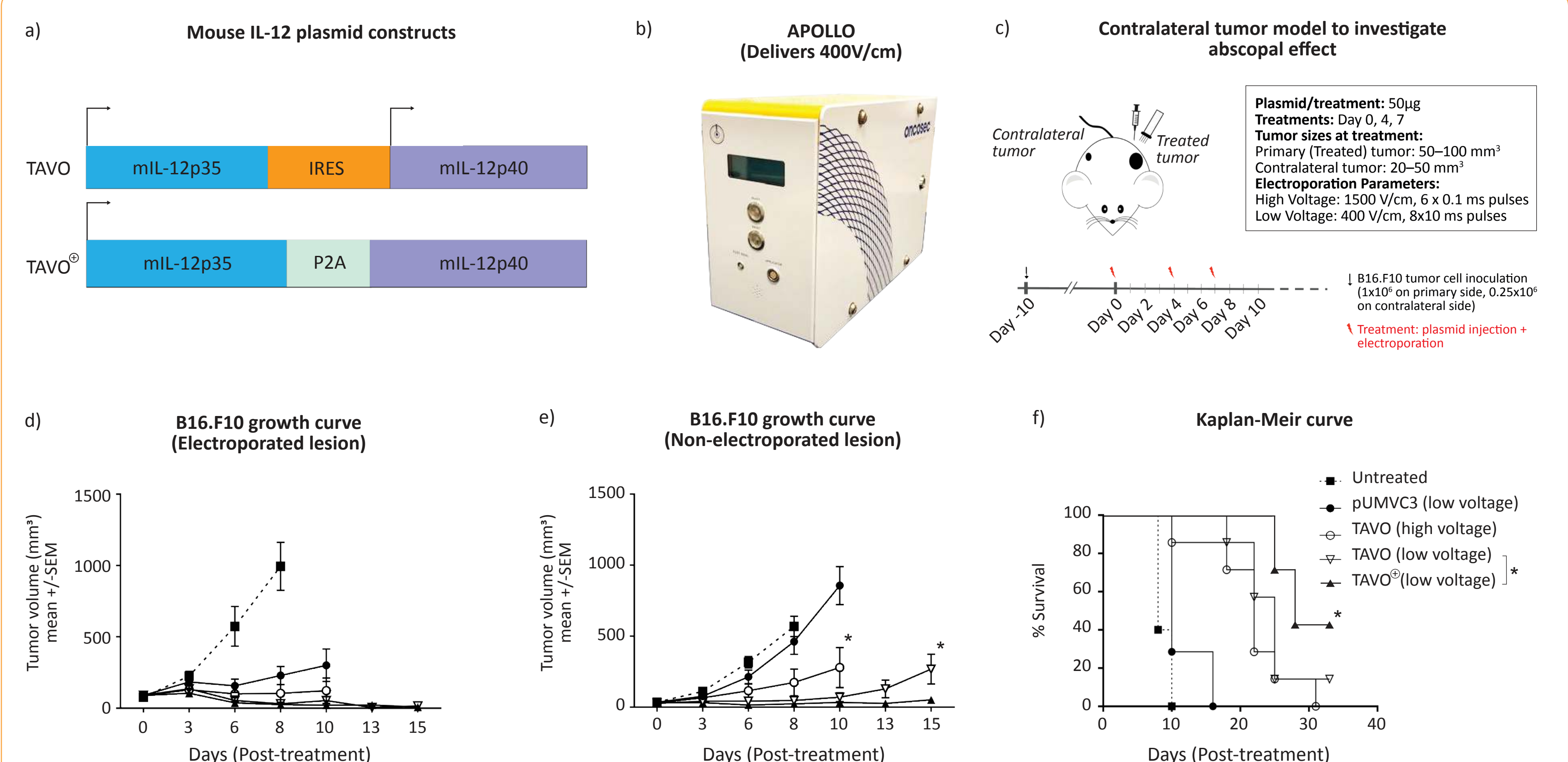


Figure 1: a) IL-12 expression constructs. **Top:** Mouse IL-12 plasmid TAVO (mIL-12p35-IRES-mIL-12p40); **Bottom:** P2A-linked bicistronic IL-12 plasmid TAVO[®] (mIL-12p35-P2A-mIL-12p40). **b)** Schematic of Oncosec's Low Voltage generator (APOLLO). **c)** Contralateral tumor model: B16.F10 or CT26 cells were implanted on both flanks of C57Bl/6J or BALB/c, 6 to 8-week-old female mice at different densities (1 million cells on left flank and 0.25 million cells on the right). Lesions were electroporated on days 0, 4, 7. Tumor volumes were calculated as follows Length x Width²/2. **d)** Growth of primary (electroporated) and **e)** contralateral B16.F10 lesions after intratumoral electroporation of 50ug TAVO under high voltage conditions (1500V/cm; open circle), low voltage conditions (400V/cm; open inverted triangle), TAVO[®] (solid triangle) and Empty vector (pUMVC3; solid circle) under low voltage conditions (400V/cm) and no treatment (solid square) are shown. n=10; statistical significance determined using two-way ANOVA with Bonferroni correction, *P < 0.0001. **f)** Kaplan-Meier curve. *P < 0.05; Gehan-Breslow-Wilcoxon test.

P2A-linked plasmid 'TAVO[®]-CXC' expresses immunologically relevant levels of functional IL-12p70 and CXCL9

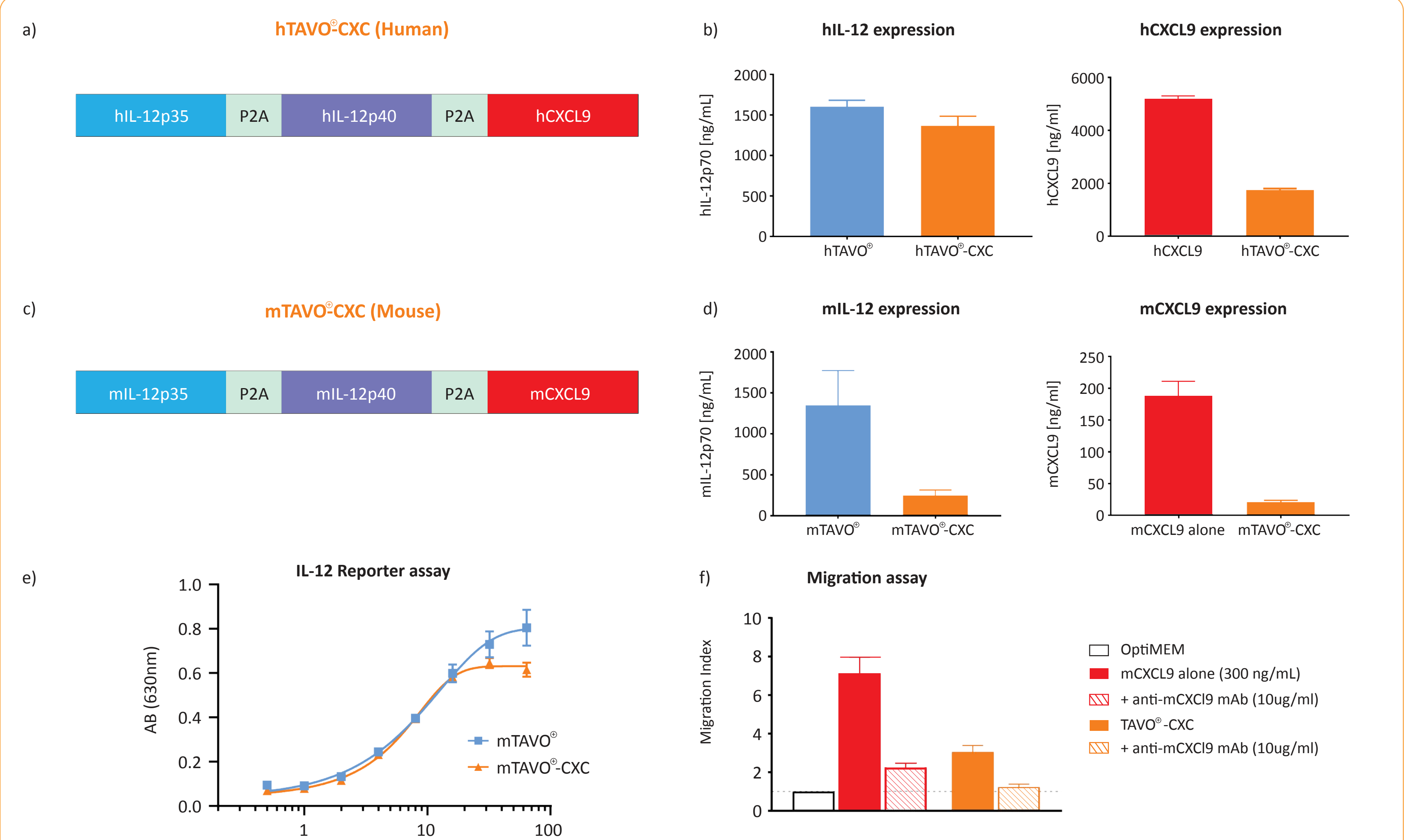


Figure 2: a) Human TAVO[®]-CXC construct (hIL-12p35-P2A-hIL-12p40-P2A-hCXCL9). **b) Left panel:** Amount of hIL-12p70 secreted by HEK293 cells transiently transfected with empty vector (Tfx control), human TAVO[®], or human TAVO[®]-CXC constructs (96hr harvest; n=5); hIL-12p70 DuoSet ELISA DY1270. **Right panel:** Amount of hCXCL9 secreted by HEK293 cells following transient transfection with Tfx control, human CXCL9, or human TAVO[®]-CXC (96hr harvest; n=5); hCXCL9 DuoSet ELISA DY392. **c)** Mouse TAVO[®]-CXC construct (mIL-12p35-P2A-mIL-12p40-P2A-mCXCL9). **d) Left panel:** Amount of mL-12p70 secreted by HEK293 cells transiently transfected with Tfx control, mouse TAVO[®], or mouse TAVO[®]-CXC constructs (96hr harvest; n=3-4); mL-12p70 DuoSet ELISA DY419. **Right panel:** Amount of mCXCL9 secreted by HEK293 cells following transient transfection with Tfx control, mouse CXCL9 and mouse TAVO[®]-CXC constructs (96hr time point; n=3); mCXCL9 DuoSet ELISA DY492. **e)** HEK-blue IL-12 cells (Invivogen HKB-IL12) produce secreted alkaline phosphatase upon IL-12p70 agonist signaling. Graph shows dose-response to mL-12p70 from transiently transfected HEK293 cells with mouse TAVO[®] or mouse TAVO[®]-CXC constructs. Both constructs encode biologically active IL-12. **f)** Transfection-derived mouse CXCL9 induced chemotaxis of SIINFEKL-pulsed (24hr @ 1ug/mL, 72hr recovery) OT-I splenocytes through polycarbonate membranes with 5.0-micron pores (Costar 3421). Migration index is defined as the number of observed chemotactic cells after 2.5 hours at 37°C, normalized to the number of cells that passively migrated through the membrane in the OptiMEM negative control. Abrogation of chemotaxis was observed with the pre-incubation of anti-mCXCL9 neutralizing monoclonal antibody (BioXcell BE0309).

Intratumoral CXCL9 synergizes with IL-12 to modulate the tumor microenvironment, expand antigen-specific T cells, and control contralateral tumor growth in a CT26 syngeneic mouse model

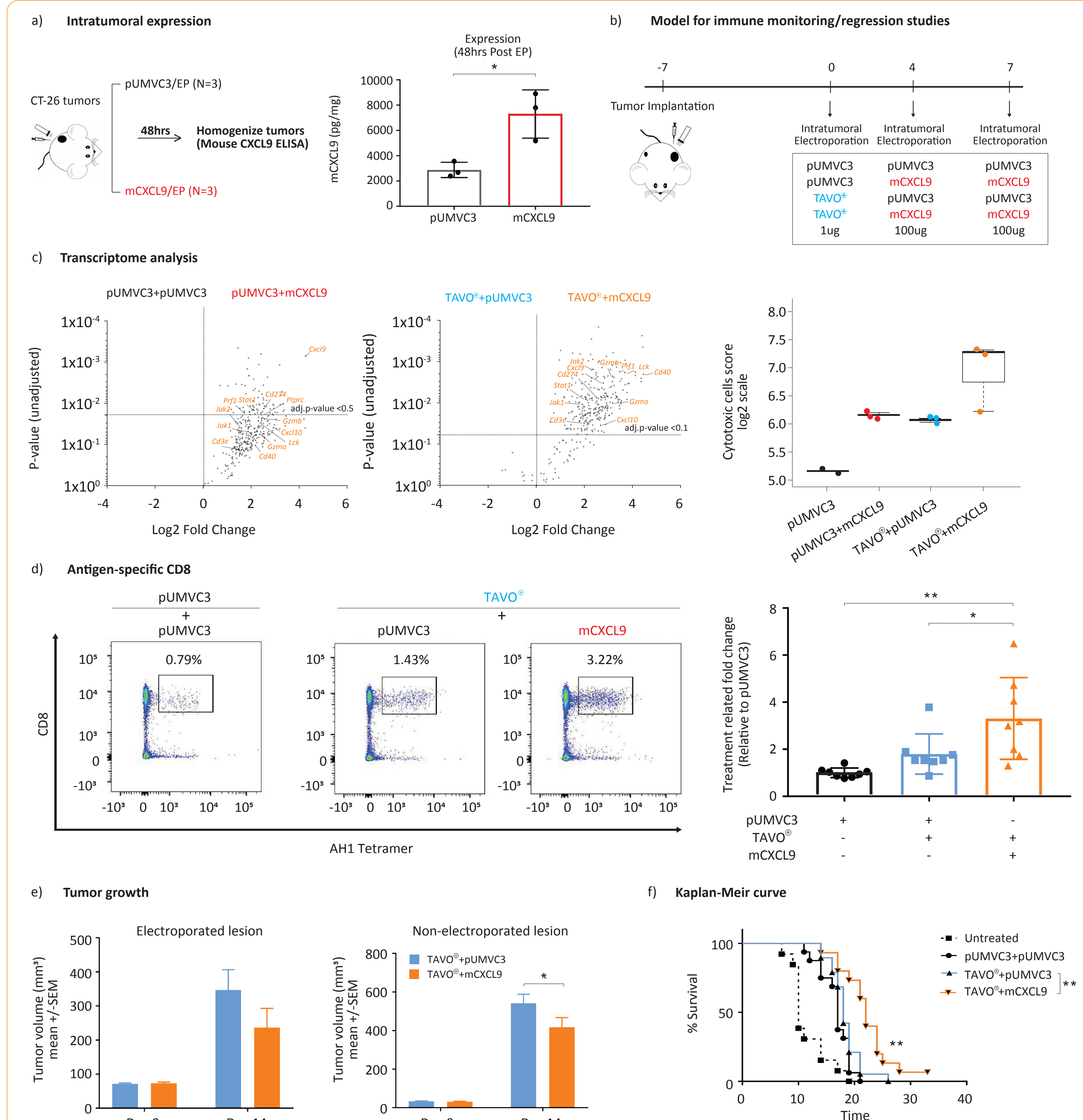


Figure 3: a) Model to evaluate intratumoral expression post electroporation. Intratumoral expression of mCXCL9 was confirmed using ELISA for mCXCL9 (DuoSet ELISA DY392) 48hrs post-electroporation in tumor lysates from mice bearing CT26 tumors (n=3; *P < 0.05; T test with Welch correction). **b)** Schematic showing intratumoral treatment regimen for combination therapy (TAVO[®]+ mCXCL9) to assess tumor regression and monitor immune response in CT26 tumor bearing mice. Single tumor model for NanoString analysis and flow based assays or a contralateral model for regression and survival studies were performed by electroporating with suboptimal dose of TAVO[®] (1 ug on Day 0) followed by 100ug of either mCXCL9 or pUMVC3 on days 4 and 7. Tumor and splenocytes were harvested 2 days after last EP (i.e. Day 9) for NanoString and flow based analysis. Alternatively, tumor volumes were measured three times a week for regression/survival studies. **c)** Gene expression changes in electroporated CT26 lesions were assessed by NanoString nCounter[®] technology. **Left panel:** Volcano plots displaying p-values and log₂ fold change for each gene. Genes differentially expressed with treatment (mCXCL9 alone or in combination with TAVO[®]; left and right respectively) have a positive value on the x axis. Horizontal lines indicate False Discovery Rate (FDR) thresholds. **Right panel:** 'Cytotoxic immune cells' cell type scores. Each cell type's score (Log₂ scale) has been centered to have mean 0. **d)** Flow cytometric analysis of splenocytes from mice treated with groups mentioned in b. **Left panel:** Antigen specific AH1⁺ CD8⁺ T cells measured via tetramer analysis (Immudex). Cells are gated on Singlets-Live-CD3⁺ CD4⁺ splenocytes. **Right panel:** Fold increase in the number of AH1⁺ CD8⁺ T cells compared to empty vector control (N=2 independent experiments with 3-5 animals/group; * P < 0.05, ** P < 0.005; One way ANOVA). **e)** Growth of primary (electroporated, left panel) and contralateral (right panel) CT26 lesions after intratumoral treatment with TAVO[®]+ pUMVC3 (blue) and TAVO[®]+ mCXCL9 (orange) are shown. At 14 days post treatment, contralateral tumors from the TAVO[®]+ mCXCL9 cohort were significantly smaller (n = 2 independent experiments with 8-10 animals/experiment, statistical significance determined using 2way ANOVA * p < 0.05). **f)** Kaplan-Meier curves (** P < 0.005; log-rank (Mantel-Cox) test).

P2A-linked plasmid 'TAVO[®]-αCD3' demonstrates robust expression of IL-12p70 and αCD3 *in vitro*

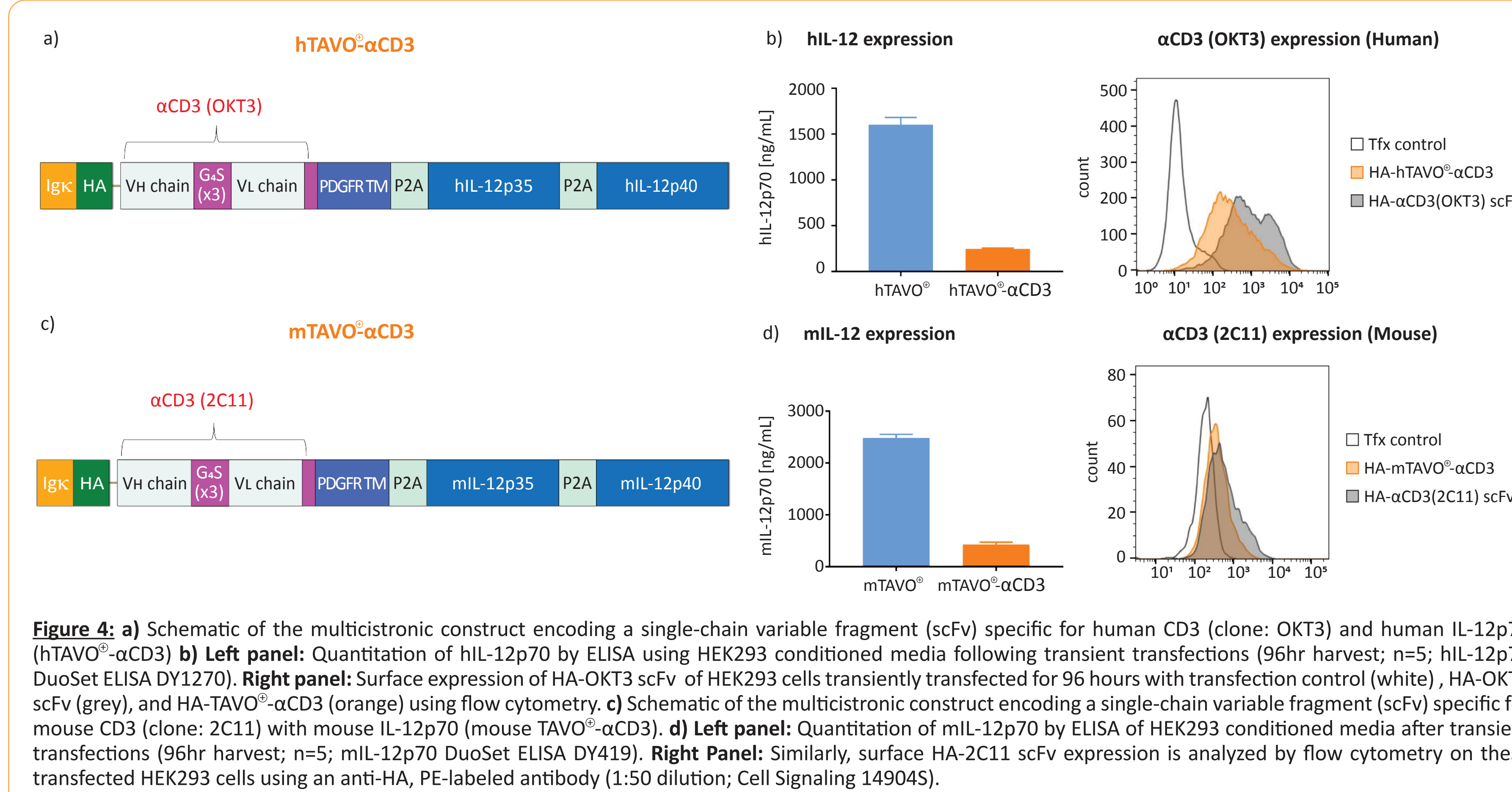


Figure 4: a) Schematic of the multicistronic construct encoding a single-chain variable fragment (scFv) specific for human CD3 (clone: OKT3) and human IL-12p70 (TAVO[®]-αCD3). **b) Left panel:** Quantitation of hIL-12p70 by ELISA using HEK293 conditioned media following transient transfections (96hr harvest; n=5); hIL-12p70 DuoSet ELISA DY1270. **Right panel:** Surface expression of HA-OKT3 scFv of HEK293 cells transiently transfected for 96 hours with transfection control (white), HA-OKT3 scFv (grey), and HA-TAVO[®]-αCD3 (orange) using flow cytometry. **c)** Schematic of the multicistronic construct encoding a single-chain variable fragment (scFv) specific for mouse CD3 (clone: 2C11) with mouse IL-12p70 (mouse TAVO[®]-αCD3). **d) Left panel:** Quantitation of mL-12p70 by ELISA of HEK293 conditioned media after transient transfections (96hr harvest; n=5); mL-12p70 DuoSet ELISA DY419. **Right Panel:** Similarly, surface HA-2C11 scFv expression is analyzed by flow cytometry on these transfected HEK293 cells using an anti-HA, PE-labeled antibody (1:50 dilution; Cell Signaling 149045).

Intratumoral membrane-bound αCD3 scFv expression leads to polyclonal T cell expansion and antigen-specific killing *in vivo*

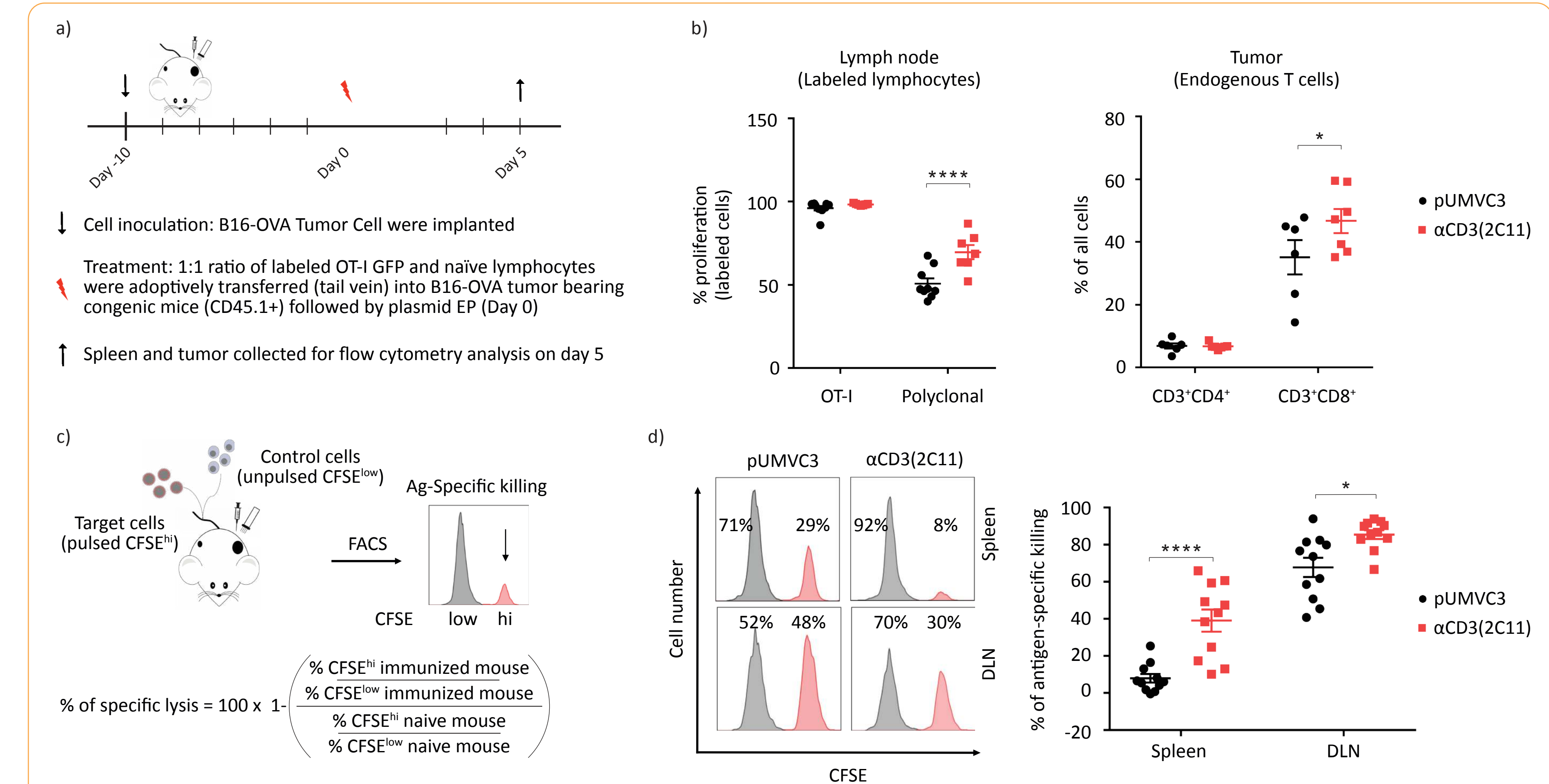


Figure 5: a) Experimental model to evaluate polyclonal T cell expansion: OT1-GFP and naïve lymphocytes (both labeled with BlueTrace Tracker) were mixed 1:1 and adoptively transferred (tail vein) to B16-OVA tumor bearing mice. Tumors were then electroporated with either αCD3(2C11) or empty vector (pUMVC3) (Day 0). Spleen, lymph node and tumor were harvested 5 days post EP. **b) Left panel:** % proliferation of adoptively transferred lymphocytes (analyzed for CFSE intensity) in the draining lymph node 5 days post EP was assessed by flow cytometry. **Right panel:** Flow cytometry analysis of tumor infiltrating endogenous T cells post intratumoral electroporation of αCD3(2C11) (n=7-8, Results are shown from 2 pooled independent experiments). *P < 0.05, **P < 0.01, ****P < 0.0001; Two-way ANOVA. **c)** Experimental design for *in vivo* cytotoxic T cells killing assay (CTL assay): Syngeneic lymphocytes as target cells were pulsed with 2ug/ml SIINFEKL peptide labeled with 1μM CFSE. Unpulsed cells (control) were labeled with 0.1μM CFSE. B16-OVA bearing mice were electroporated with pUMVC3 or αCD3(2C11) and one day later, pulsed target cells and unpulsed cells (1:1) were adoptively transferred. 18 hours after adoptive transfer, spleens and draining lymph nodes were collected and analyzed. **d)** Measured by flow cytometric analysis of spleens and draining lymph nodes demonstrating significant antigen-specific killing. The killing is described by the percentage of specific target cells killed (i.e., (1 - target/control) × 100), (n=11, Results are shown from 2 pooled independent experiments). *P < 0.01, ****P < 0.0001; Two-way ANOVA.

Intratumoral αCD3 augments anti-tumor effect of TAVO[®] in a B16.F10 contralateral tumor model

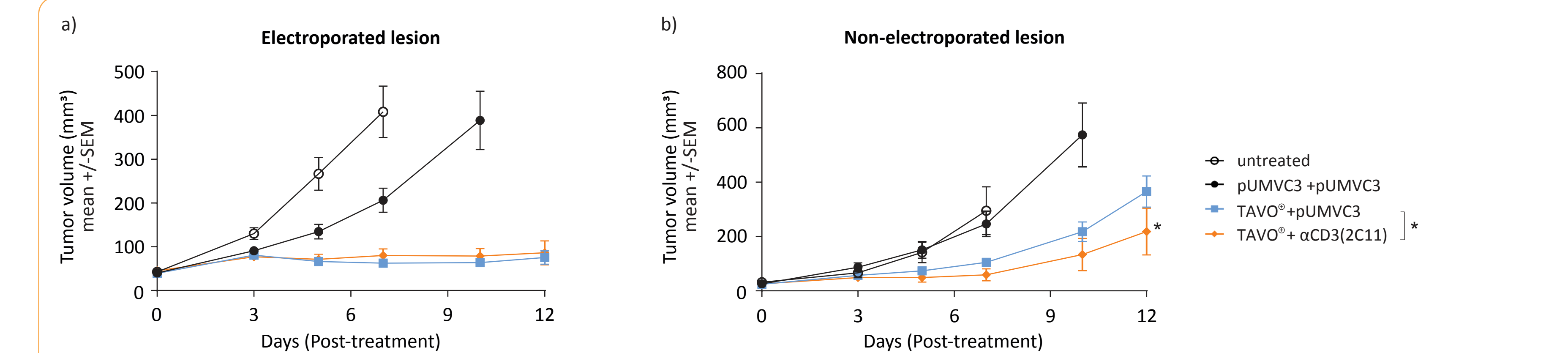


Figure 6: a) Growth of primary (electroporated) and b) contralateral (non-electroporated) B16.F10 lesions after treatment with a suboptimal dose of hTAVO[®]/EP (2ug) on day 0 in combination with hT-pUMVC3 (100ug) (days 3, 5; blue) or hT-Anti CD3(2C11) (days 3, 5; orange), hT-pUMVC3 (2ug) on day 0 + hT-pUMVC3/EP (100ug) (days 3, 5; black) was used as an empty vector control. Untreated mice were not electroporated/injected with any plasmid (black, open circle). Two-way ANOVA was used for statistical analysis. *P < 0.05

Combining TAVO[®]-CXC with TAVO[®]-αCD3 ('SPARK') delays tumor growth in a contralateral tumor model.

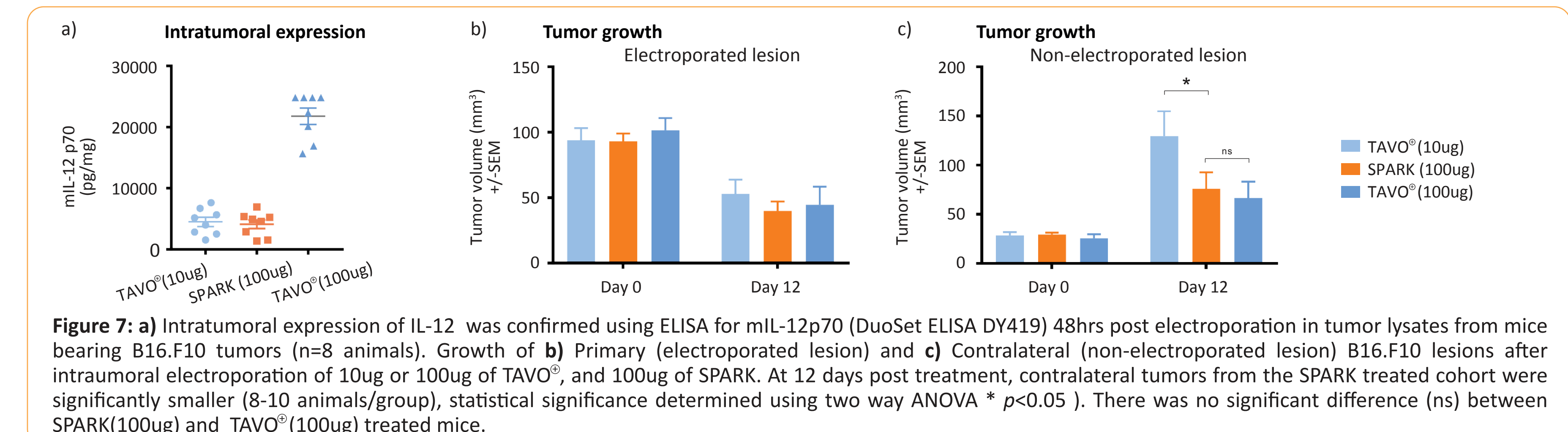
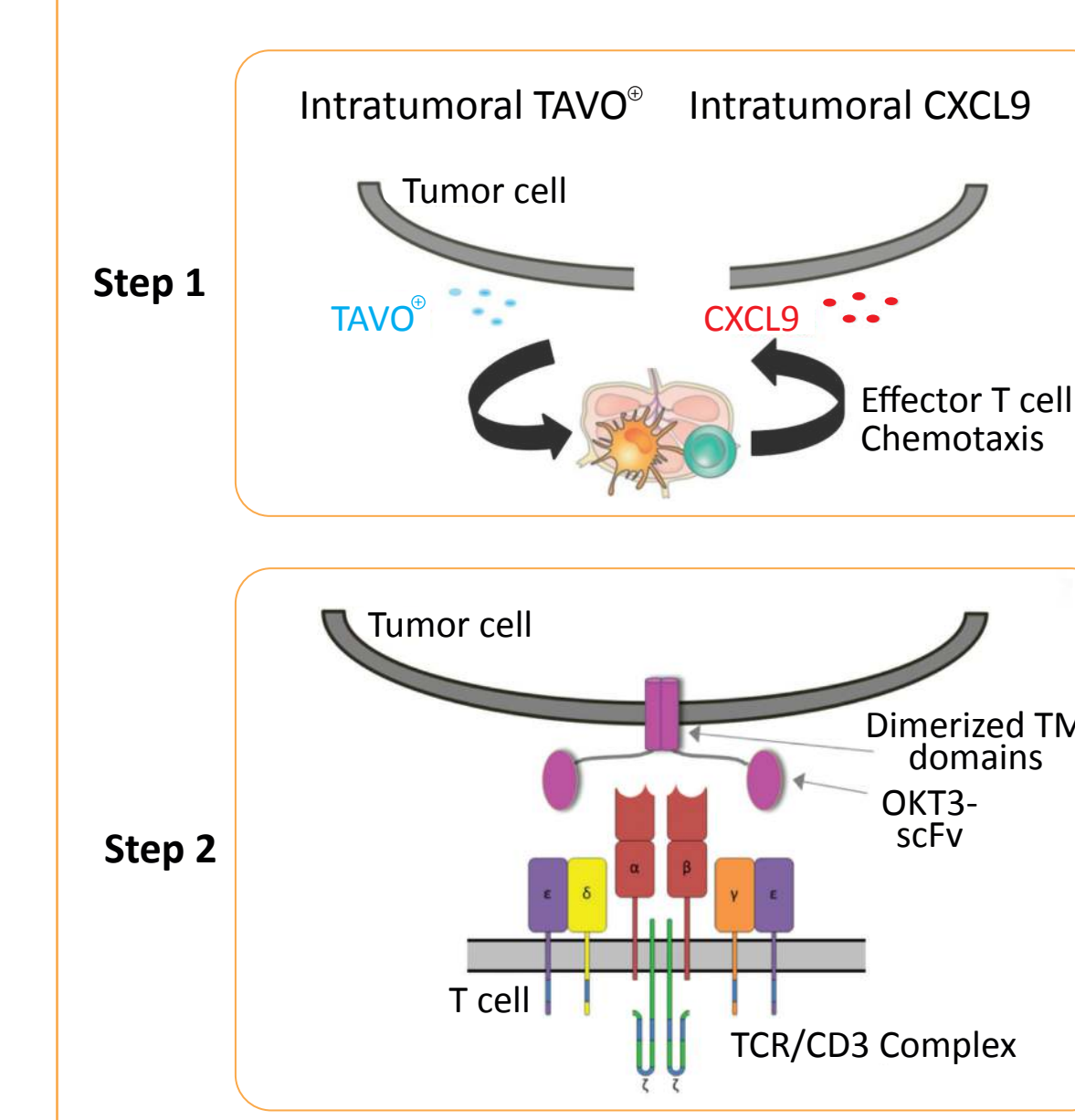


Figure 7: a) Intratumoral expression of IL-12 was confirmed using ELISA for mL-12p70 (DuoSet ELISA DY419) 48hrs post electroporation in tumor lysates from mice bearing B16.F10 tumors (n=8 animals). Growth of b) Primary (electroporated lesion) and c) Contralateral (non-electroporated lesion) B16.F10 lesions after intratumoral electroporation of 10ug or 100ug of TAVO[®], and 100ug of SPARK. At 12 days post treatment, contralateral tumors from the SPARK treated cohort were significantly smaller (8-10 animals/group), statistical significance determined using two way ANOVA * p < 0.05). There was no significant difference (ns) between SPARK(100ug) and TAVO[®](100ug) treated mice.

Summary and Conclusion

Proposed Mechanism of Action: SPARK



Conclusion

- Novel pIL-12-P2A plasmid delivered with low voltage electroporation parameters leads to improved contralateral (systemic) anti-tumor response.
- Plasmid encoding both IL-12 and the effector T cell chemokine, CXCL9 (TAVO[®]-CXC), is functionally active *in vitro* as shown by an IL-12 responsive HEK reporter line and transwell chemotaxis assays.
- Intratumoral CXCL9/EP when combined with intratumoral IL-12/EP:
 - Positively modulates the TME (infiltration of cytotoxic cells demonstrated by NanoString analysis of CT26 tumors)
 - Results in generation of antigen-specific CD8⁺ CTL (AH1⁺CD8 in CT26 MODEL)
 - Augments abscopal response of TAVO[®] (CT26 contralateral tumor model).
- Membrane bound αCD3 expression increases both antigen-specific and polyclonal T cells responses, (endogenous or adoptively transferred), demonstrated by *in vivo* CTL and proliferation assays.
- TAVO[®]-αCD3 demonstrates improved abscopal anti-tumor response compared to TAVO[®] alone in a B16.F10 tumor model
- Finally, Combination of IL-12/CXCL9 with anti-CD3 delivered by electroporation (collectively called 'SPARK') lead to regression of both treated and untreated tumors in B16.F10 mouse syngeneic tumor model

Summary

SPARK represents a significant advancement in cytokine-based immunotherapy and Oncosec plans to file an Investigational New Drug application for this product by the end of 2019.